By tuning the coefficient to 0.5, it shows better agreement with the experimental data. Because of insufficient measurement data along the reattachment, there is still some uncertainty in the peak Stanton value in that region. Nevertheless, this certainly is not the means to solve the problem. The main difficulty in this problem is to establish a physical transition model at the reattachment. Moreover, applying an incorrect transition model at the reattachment renders an incorrect onset of separation upstream, as shown in Fig. 5 at $\bar{X} = 0.64$.

Conclusion

The prediction of relaminarization with the SA model has been demonstrated with an axisymmetric configuration that has not been validated by the authors of the model in Ref 1. The sensitivity of the closure coefficients is highlighted, and more research is required to validate the SA model before it can be used universally with any configuration. Because of the lack of a physical transition model in the SA model, care has to be taken in the uncertainty in the prediction of transition onset and duration with this model. In addition, the compressibility effect has not been taken into account in this model.

References

[1] Spalart, P. R., and Allmaras, S. R., "A One-Equation Turbulence Model for Aerodynamic Flows," AIAA Paper 92-0439, Jan. 1992.

[2] Baldwin, B. S., and Lomax, H., "Thin Layer Approximation and Algebraic Model for Separated Turbulent Flows," AIAA Paper 78-0257, Jan. 1978.

[3] Wong, H., "Hypersonic Flow over a Hyperboloidal-Flare," *Proceedings of the First Europe–US High Speed Flow Field Database Workshop Part 2*, Italian Aerospace Research Centre (to be published).

[4] Granville, P. S., "Baldwin–Lomax Factors for Turbulent Boundary Layers in Pressure Gradients," *AIAA Journal*, Vol. 25, No. 12, 1987, pp. 1624–1627.

[5] Krogmann, P., "Calibration and Validation Measurements in the Ludwieg Tube Tunnel B (RWG)," DLR Göttingen, Rept. ESA/CNES HT-TR-E-1-301-DGLR, Göttingen, Germany, Aug. 1995.

C. G. Speziale
Associate Editor

Wake Generation Compressibility Effects in Unsteady Aerodynamics

Ronald J. Epstein* and Donald B. Bliss†
Duke University, Durham, North Carolina 27708-0300

Introduction

THE phenomena of wake generation and evolution are the subject of continued research[1–8] and development. When dealing with either conventional fixed-wing aircraft or rotorcraft, the wake formation and subsequent dynamics are important issues. The behavior of the wake can profoundly affect aerodynamic loading, induced wash, and aerodynamic noise. In some situations the assumptions of an incompressible (constant-density) wake flow facilitates aerodynamic modeling. This assumption is particularly beneficial for three-dimensional, free-wake analysis, where motion and deformation of the wake under its own influence is to be determined.[6,7] Free-wake analysis is commonly used in rotorcraft aerodynamic models. Typically, the wake is discretized into vortex elements connected to form vortex filaments and/or vortex sheets. The velocity field from these elements is computed using the Biot–Savart law, which restricts the validity of the wake representation to incompressible constant-density flow. That the wake convects with the surrounding fluid and induces flow velocities that have very low Mach numbers appears to support the accuracy of the incompressible flow assumption. It is, therefore, not unusual to find rotorcraft aerodynamic analyses that embody compressibility effects in the blade aerodynamics model but utilize an incompressible free-wake analysis.

A criticism of this approach is that, although the wake-induced velocities may be low, the relative velocities between the wake and the generating blade, and subsequent blades the wake may encounter, may correspond to relatively high subsonic Mach numbers. During the unsteady wake generation process, waves generated both on the airfoil and in the wake itself travel both upstream and downstream, and the finite propagation speed (especially the slower upstream wave) may introduce significant phase delays in comparison with an incompressible case that has infinite wave speed. The implications of coupling an incompressible wake to a compressible blade aerodynamics analysis have not been systematically explored, even though this approach has been repeatedly undertaken in practice as an expedient to the formulation of a complex problem.

The present research illustrates the role of wake compressibility for the relatively simple case of a wake generated by a two-dimensional unsteady airfoil, as a first step toward exploring the effect of the wake incompressibility assumption. Even this relatively simple case will be seen to provide considerable physical insight. From this, a criterion for wake compressibility is derived. The derivation, from fundamental physical principles, also includes a discussion of the fundamental length and timescales that appear in the problem.

To illustrate the derived wake compressibility criterion, numerical results are presented for a model unsteady compressible aerodynamic calculation, namely a flat-plate airfoil encountering a harmonic nonuniform inflow. This is a compressible form of the von Kármán–Sears problem.[9,10] Through this simple example, it is demonstrated that wake compressibility can indeed have a profound effect on unsteady aerodynamic and aeroacoustic calculations.[11,12] It is also shown that only a small portion of the wake, that which is closest to the trailing edge of the lifting surface, is important with regard to wake compressibility. Therefore, the criterion derived can be regarded as a correction to existing wake analysis schemes as opposed to a replacement for them and, as demonstrated, can be effectively used as such.

Wake Compressibility Criterion

Consider a two-dimensional wing section (Fig. 1a), translating in the $-x$ direction with velocity V_∞ subject to an unsteady excitation. The excitation can be due to unsteady heave, pitch, or gust and is not limited to the frequency domain. An unsteady wake is, therefore, shed from the trailing edge of the wing section. The wake is composed of both positive and negative vorticity, as shown schematically in Fig. 1a. The sign and magnitude of the vorticity in the wake acts as an effective fluidic memory for the unsteady changes of vorticity, upwash, and pressure on the surface of the wing section and must satisfy Kelvin's theorem.

This Note investigates the aeroacoustic aspects of the wake as it is generated at the trailing edge. It is assumed that the wake is continuously shed both temporally and spatially. Therefore, in any small increment of time, a small increment of wake is shed and convects from the trailing edge. The detailed viscous mechanism of the shedding process[13] is not addressed. Rather, the global aeroacoustics of the wake inception is investigated.

Looking at Fig. 1a, consider a small increment of wake being shed. Simultaneously, a sound wave is emitted at the trailing edge from the unsteady disturbance induced by a newly shed wake increment. The sound wave is generated by the final adjustment of the flowfield at the trailing edge. In terms of potential flow or panel methods,[14–19] this is the last adjustment made in the surface potential strength distribution (source or doublet), at the trailing edge, before the local jump in potential is shed into the wake. The value of the jump in potential at the trailing edge is then convected downstream in the wake. This is equivalent to satisfying Kelvin's theorem.

Received July 12, 1996; revision received June 18, 1998; accepted for publication July 8, 1998.

*Research Assistant Professor, Department of Mechanical Engineering and Material Science, School of Engineering; currently Project Engineer, Phantom Works, The Boeing Company, Mailcode S1067126, P.O. Box 516, St. Louis, MO 63166-0516. Member AIAA.

†Associate Professor, Department of Mechanical Engineering and Material Science, School of Engineering. Member AIAA.

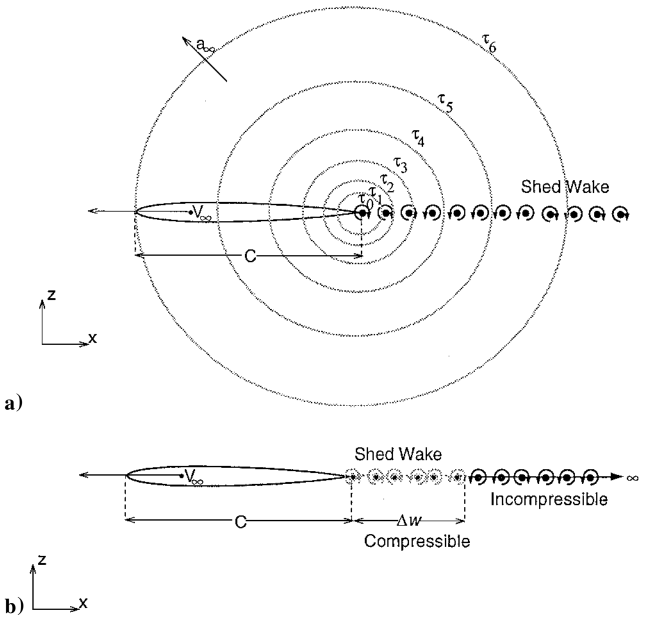

Fig. 1 Schematic of a translating wing section and shed wake, where C is the chord, V_∞ is the wing section velocity, a_∞ is the speed of sound, and τ_n are the n preceding time steps.

The sound wave emitted from the trailing edge travels both upstream and downstream ($\pm x$ directions) at the speed of sound a_∞. Therefore, relative to the surface of the wing section, which is traveling at V_∞ in the negative x direction, the upstream sound wave will travel at a net velocity

$$V_{\text{net}} = a_\infty - V_\infty \tag{1}$$

Therefore, the time required for a sound wave emitted from the trailing edge to travel to the leading edge can be approximated by the time required for a sound wave to travel one linear chord length C upstream relative to the freestream; in Fig. 1a this is shown as the wave front emitted from the trailing edge at τ_0 ($\tau_0 < \tau_6$), which reaches the leading edge at τ_6. Therefore, if the chord length is divided by the upstream speed of the sound waves emitted from the trailing edge, Eq. (1), this gives

$$\tau_C = \frac{C}{a_\infty - V_\infty} \tag{2}$$

which is the time needed for a sound wave to travel upstream one chord length relative to the freestream velocity. In terms of Fig. 1a, $\tau_C = \tau_6 - \tau_0$.

During τ_C, the wake increment that was shed at time τ_0 has convected downstream a distance Δw, which can be simply calculated by multiplying τ_C by the convection velocity V_∞, which gives

$$\Delta w = \tau_C \times V_\infty = \frac{C V_\infty}{a_\infty - V_\infty} \tag{3}$$

and can be rewritten as

$$\Delta w / C = M_\infty / (1 - M_\infty) \tag{4}$$

where $M_\infty = V_\infty / a_\infty$. A similar expression was stated by Rowe and Cunningham[20] for time-harmonic problems without detailed derivation. Equation (4) gives a characteristic length scale associated with compressible wake formation, where Δw is given as a function of M_∞ and C. Note that Δw can be very small when compared with the net wake length. A reduced frequency related to the compressible wake formation is given by the reciprocal of Eq. (2) as $1/\tau_C$.

It is also interesting to point out that, at $M_\infty = 0$, $\Delta w = 0$; however, at $M_\infty = 1$, $\Delta w = \infty$, which means that downstream waves will never travel upstream. This corresponds to the hyperbolic casuality of the supersonic problem or simply that information cannot travel upstream in supersonic flow. For intermediate Mach numbers, only one or two chord lengths are needed.

Numerical Results and Discussion

To illustrate the concept, the response of a flat-plate airfoil to a nonuniform inflow (sinusoidal)[10–12,21] in linearized potential flow is considered. This is a compressible von Kármán–Sears problem. In general, the governing equation of linear, compressible, unsteady potential flow can be written as[22,23]

$$\left(1 - \frac{V_\infty^2}{a_\infty^2}\right)\frac{\partial^2 \varphi}{\partial x^2} + \frac{\partial^2 \varphi}{\partial y^2} + \frac{\partial^2 \varphi}{\partial z^2} - 2\frac{V_\infty}{a_\infty^2}\frac{\partial^2 \varphi}{\partial x \partial t} - \frac{1}{a_\infty^2}\frac{\partial^2 \varphi}{\partial t^2} = 0 \tag{5}$$

where t is time and φ the velocity potential. This equation can be solved by any suitable means; for the present work it was solved using the analytical/numerical matching boundary element method.[24–28]

Figure 2 shows the chordwise magnitude of the pressure difference distribution calculated for an airfoil subject to $C = 2b$, $kb = 2.5$, $k_r = 6.25$, and $M_\infty = 0.4$, where b is the semichord, $k = \omega / a_\infty$ is the freespace acoustic wave number, $k_r = (\omega b)/V_\infty$ is the reduced frequency, and M_∞ is the Mach number. Results were calculated using compressible unsteady aerodynamics on the flat-plate surface and each of the three following wake models: a full compressible wake model, an incompressible wake model, and a corrected incompressible wake model. Figure 2 also shows the chordwise real and imaginary parts of the pressure difference distribution. In the calculation, the inflow upwash velocity varies sinusoidially, the gust wavelength is half the chord length, and 100 boundary elements were distributed along the chord.

In the model calculations, the compressible wake model uses potential doublet solutions to Eq. (5) in the wake. The incompressible

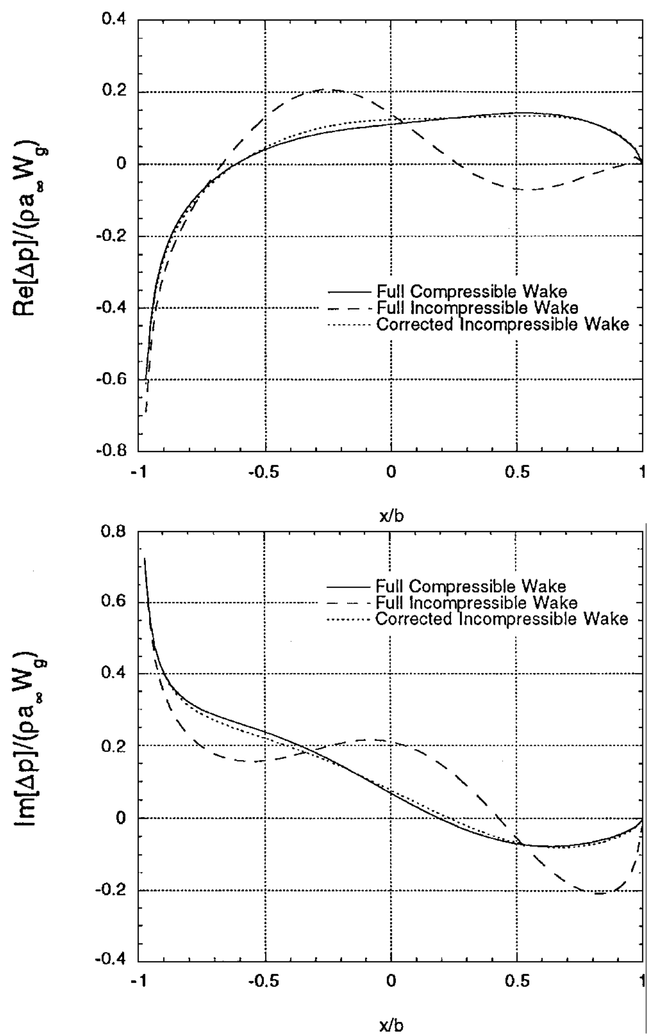

Fig. 2 Real and imaginary parts of perturbation pressure difference distribution for a flat-plate airfoil subject to nonuniform sinusoidal gust with different wake models; $kb = 2.5$, $k_r = 6.25$, $M_\infty = 0.4$, and $r_c/d_s = 1.5$.

wake model uses doublet solutions to Eq. (5) in the limit as $a_\infty \to \infty$, namely the Laplace equation. The corrected incompressible wake model is a hybrid wake with the first Δw segment of the wake modeled with doublet solutions to Eq. (5) and the rest of the wake modeled with doublet solutions to Laplace's equation, as shown in Fig. 1b.

Looking at Fig. 2, the agreement between the corrected incompressible model and the compressible model is very good. It is interesting to point out that, whereas the pressure distribution calculated with the incompressible wake differs considerably from the fully compressible calculation and the corrected incompressible, the net lift calculation (integrated pressure distribution) is not that far off.

The wake compressibility approximation outlined in this Note sheds light on several interesting and potentially useful phenomenological facts. It is significant to note that much of the physics of wake compressibility is related to wake generation. Therefore, for many subsonic flows, the physics is limited to a compact region close to the trailing edge. In terms of numerical aeroacoustics, the advantages of the wake compressibility approximation are quite pragmatic. The importance of proper wake modeling in aerodynamic/aeroacoustic applications is well known.[29] Formal treatments of compressibility have been addressed with finite volume and difference techniques; however, their applicability to routine aerodynamic design calculations is limited due to the time-intensive nature of these methods.[30] It is, therefore, not uncommon to find hybrid and semi-empirical boundary element methods used for aerodynamic design calculations in industry.[31] They are hybrid in the sense that they combine two or more boundary element schemes for an aerodynamic/aeroacoustic calculation, typically one method for wing/body aerodynamics and another for wake aerodynamics. In many codes the lifting body is modeled with a panel method (potential boundary element scheme), and the wake aerodynamics are modeled with some form of vortex element.[18] Many times these methods are calibrated with experimental data. The sophistication of the wake model varies greatly; however, many methods use a form of free-wake calculation.[6] Incompressible free-wake calculations are complex analyses and are presently still under much development and refinement.[32,33] At this point, a compressible free-wake calculation for routine design calculations is out of the scope of most research efforts, industrial and academic alike. Therefore, the compressible wake approximation outlined in this Note offers a workable engineering solution to this problem. Properly utilizing the wake compressibility criterion, an incompressible free-wake analysis can be combined with a compressible aerodynamic model, without a loss of accuracy or physical consistency.

Conclusion

The necessity for modeling unsteady compressible wake effects in compressible unsteady aerodynamics is addressed. The role of compressibility during the initial stages of wake formation is determined. It is shown that a compact portion of the wake, that which is closest to the trailing edge, is most important with regard to wake compressibility for many subsonic flows. A simple approximation is derived that determines the relative magnitude of the compressible wake length that must be used in a calculation. The approximation is based on fundamental physical principles and is relevant to compressible flow problems involving free-wake flows. The approximation is demonstrated by a numerical example, which substantiates the proposed theory and illustrates its application. The compressible wake phenomena discussed in this Note have implications for the fundamental understanding of the aeroacoustic physics of unsteady wake generation in compressible flow.

Acknowledgments

While doing this work, the first author was partially supported by a Graduate Student Researchers Program Fellowship from the NASA Langley Research Center, with Thomas F. Brooks serving as Technical Monitor.

References

[1] Betz, A., "Behavior of Vortex Systems," NACA TM-713, June 1933.

[2] Spreiter, J. R., and Sacks, A. H., "The Rolling Up of the Trailing Vortex Sheet and Its Effect on the Downwash Behind Wings," *Journal of the Aeronautical Sciences*, Vol. 18, Jan. 1951, pp. 21–32.

[3] Wetmore, J. W., and Reeder, J. P., "Aircraft Vortex Wakes in Relating to Terminal Operations," Aeronautical Research Council, TN D-1777, April 1963.

[4] Rose, R., and Dee, F. W., "Aircraft Vortex Wakes and Their Effects on Aircraft," Aeronautical Research Council, CP-795, 1965.

[5] Donaldson, C. D., and Bilanin, A. J., "Vortex Wakes of Conventional Aircraft," AGARDograph 204, May 1975.

[6] Bliss, D. B., Teske, M. E., and Quackenbush, T. R., "A New Methodology for Free Wake Analysis Using Curved Vortex Elements," NASA CR-3958, Dec. 1987.

[7] Quackenbush, T. R., and Bliss, D. B., "Free Wake Flow Field Calculations for Rotorcraft Interactional Aerodynamics," *Vertica*, Vol. 14, No. 3, 1990, pp. 313–327.

[8] Rossow, V. J., "Validation of Vortex-Lattice Method for Loads on Wings in Lift-Generated Wakes," AIAA Paper 94-1839, June 1994.

[9] von Kármán, T., and Sears, W. R., "Airfoil Theory for Nonuniform Motion," *Journal of the Aeronautical Sciences*, Vol. 5, No. 10, 1938, pp. 379–390.

[10] Amiet, R. K., "Airfoil Gust Response and the Sound Produced by Airfoil–Vortex Interaction," *Journal of Sound and Vibration*, Vol. 107, No. 3, 1986, pp. 487–506.

[11] Amiet, R. K., "High Frequency Thin-Airfoil Theory for Subsonic Flow," *AIAA Journal*, Vol. 14, No. 8, 1976, pp. 1076–1082.

[12] Atassi, H., "Unsteady Aerodynamics of Vortical Flows: Early and Recent Developments," *Symposium on Aerodynamics and Aeroacoustics*, edited by K.-Y. Fung, World Scientific, 1994.

[13] Mangler, K. W., and Smith, J. H. B., "Behavior of the Vortex Sheet at the Trailing Edge of a Lifting Wing," *Aeronautical Journal*, Vol. 74, Nov. 1970, pp. 906, 907.

[14] Hess, J., and Smith, A., "Calculation of Nonlifting Potential Flow About Arbitrary Three-Dimensional Bodies," *Journal of Ship Research*, Vol. 8, 1964, pp. 22–44.

[15] Djojodihardjo, R. H., and Widnall, S. E., "A Numerical Method for Calculation of Nonlinear, Unsteady Lifting Potential Flow Problems," *AIAA Journal*, Vol. 7, No. 10, 1969, pp. 2001–2009.

[16] Morino, L., "A General Theory of Unsteady Compressible Potential Aerodynamics," NASA CR-2464, Dec. 1974.

[17] Margason, R. J., "Subsonic Panel Methods: A Comparison of Several Production Codes," AIAA Paper 85-0280, Jan. 1985.

[18] Erickson, L. L., "Panel Methods—An Introduction," NASA TP-2995, Dec. 1990.

[19] Katz, J., and Plotkin, A., *Low Speed Aerodynamics, From Wing Theory to Panel Methods*, Series in Aeronautical and Aerospace Engineering, McGraw–Hill, New York, 1991, Chap. 9.

[20] Rowe, W. S., and Cunningham, H. J., "On the Convergence of Unsteady Generalized Aerodynamic Forces," *Journal of Aircraft*, Vol. 21, No. 6, 1984, pp. 420–427.

[21] Amiet, R. K., "On the Second-Order Solution to the Sears Problem for Compressible Flow," *Journal of Fluid Mechanics*, Vol. 254, Sept. 1993, pp. 213–228.

[22] Garrick, I. E., *Nonsteady Wing Characteristics, Aerodynamics of Aircraft Components at High Speed*, Vol. 7, Princeton Univ. Press, Princeton, NJ, 1957, Sec. F.

[23] Ashley, H., and Landahl, M., *Aerodynamics of Wings and Bodies*, Dover, Mineola, NY, 1965, Chap. 2.

[24] Epstein, R. J., "A Novel Boundary Element Method Using Analytical/Numerical Matching for Aerodynamics, Acoustics and Aeroacoustics," Ph.D. Dissertation, Dept. of Mechanical Engineering, Duke Univ., Durham, NC, May 1996.

[25] Bliss, D. B., and Epstein, R. J., "Novel Approach to Aerodynamic Analysis Using Analytical/Numerical Matching," *AIAA Journal*, Vol. 34, No. 11, 1996, pp. 2225–2232.

[26] Bliss, D. B., and Epstein, R. J., "A Novel Approach to Aerodynamic Analysis Using Analytical/Numerical Matching," *Proceedings of the AIAA 13th Applied Aerodynamics Conference* (San Diego, CA), AIAA, Washington, DC, 1995, pp. 626–639.

[27] Epstein, R. J., and Bliss, D. B., "An Aeroacoustic Boundary Element Method Using Analytical/Numerical Matching," *Proceedings of the CEAS/AIAA 1st Joint Aeroacoustics Conference* (Munich, Germany), 1995.

[28] Epstein, R. J., and Bliss, D. B., "Novel Acoustic Boundary Element Calculations Using Analytical/Numerical Matching Applied to Three-Dimensional Fluid Loaded Plate," *Proceedings of FORUM ACUSTICUM—The 1st Convention of the European Acoustics Association* (Antwerp, Belgium), 1996.

[29] Caradonna, F. X., Laub, G. H., and Tung, C., "An Experimental Investigation of the Parallel Blade–Vortex Interaction," *Proceedings of the 10th European Rotorcraft Forum* (The Hague, The Netherlands), 1984.

[30] Prichard, D., Burley, C., and Boyd, D. D., Jr., "Computational

Techniques for Improved Blade Vortex Interaction Modeling," *Proceedings of the 51st Annual Forum of the American Helicopter Society* (Fort Worth, TX), 1995.

[31]Johnson, W., *Helicopter Theory*, Princeton Univ. Press, Princeton, NJ, 1980, Chap. 1.

[32]Miller, W., "Analytical/Numerical Matching and Periodic Inversion: Two Advances in Free Wake Analysis," Ph.D. Dissertation, Dept. of Mechanical Engineering, Duke Univ., Durham, NC, May 1990.

[33]Bliss, D. B., and Miller, W. O., "Efficient Free Wake Calculations Using Analytical/Numerical Matching," *Journal of the American Helicopter Society*, Vol. 38, No. 2, 1993, pp. 878, 879.

S. Glegg
Associate Editor

Two-Way Coupled Gas-Particle Systems in an Axisymmetric Ramjet Combustor

E. J. Chang* and K. Kailasanath†
U.S. Naval Research Laboratory, Washington, D.C. 20375
and
S. K. Aggarwal‡
University of Illinois at Chicago, Chicago, Illinois 60680

Introduction

FOR a variety of reasons, in many multiphase flow applications, tracking the dispersed phase in a Lagrangian manner may be desirable. Here individual particle trajectories are calculated as they are carried by the gas phase in the system.[1–4] However, because of the high numerical cost of tracking large numbers of particles, these studies have necessarily been kept at relatively low seeding and mass fraction levels. To reach higher seeding levels, using virtual particle methods where each computational, or tracked, particle actually represents a group of particles of the same size has been necessary.[5] Calculation of energy and momentum transfer between phases is then based on the entire group instead of just the carrier particle. Using such a method allows a high mass loading to be obtained without the necessary computational expense of tracking every particle in the system. However, the accuracy of the results obtained using this technique is a matter of concern.[6]

This Note extends our previous efforts on the simulation of particle dynamics in the confined geometry of an idealized ramjet combustion system.[3,4] In that work we neglected the effect of the particles on the fluid flow. We now take up the issue of return momentum and energy effects from the particles to the gas phase of the flow. The inclusion of such return effects is critical to the development of reliable predictive tools for transient, multiphase flows in propulsion systems such as ramjets. In a situation such as that considered here, with particles injected as a narrow stream, the use of virtual particles may be called into question. Artificially high mass loadings may arise within a computational cell as the true distribution of particles in space is neglected and replaced by a carrier particle. Thus, return effects that may be distributed over several computational cells as particles are dispersed in the flow may, in fact, be represented as a single point force when using the virtual particle method. Results are presented from simulations with and without virtual particles at the same mass loading levels in an effort to determine how accurately the use of virtual particles represents the coupled gas-particle system.

Numerical Model

The flow into a central dump ramjet combustor is computed by solving the compressible, time-dependent, conservation equations for mass, momentum, and energy in an axisymmetric geometry. These equations are given as

$$\frac{\partial \rho}{\partial t} = -\nabla \cdot (\rho \boldsymbol{U}) \tag{1}$$

$$\frac{\partial (\rho \boldsymbol{U})}{\partial t} = -\nabla \cdot (\rho \boldsymbol{U}\boldsymbol{U}) - \nabla p + \boldsymbol{S}_v \tag{2}$$

$$\frac{\partial E}{\partial t} = -\nabla \cdot (E\boldsymbol{U}) - \nabla \cdot p\boldsymbol{U} + S_E \tag{3}$$

where $E = e + \frac{1}{2}\rho \boldsymbol{U}^2$ and $e = p/(\gamma - 1)$; ρ, p, e, $\boldsymbol{U}$, and γ are the density, pressure, internal energy, velocity, and specific heat ratio, respectively. $\boldsymbol{S}_v$ and S_E are momentum and energy source terms from the particle, or dispersed, phase, which accounts for mass loading effects. To solve these equations, the flux-corrected transport (FCT) algorithm,[7] a conservative, monotonic algorithm with fourth-order phase accuracy, is employed. Further details on the numerical approach used can be found in Ref. 3.

The geometric configuration used is shown in Fig. 1 and is representative of a generic ramjet propulsion system. A cylindrical jet with a prescribed mean velocity of 100 m/s flows through an inlet of diameter $D = 6.35$ cm into a cylindrical combustion chamber of larger diameter $2D$. An annular exit nozzle at the end of the chamber is modeled to produce choked flow and forces the flow to become sonic at the exit throat. The mass inflow rate is 0.78 kg/s, and the initial chamber pressure is 188 kPa. A fixed 60×120 computational grid is used with fine zones near the entrance to the combustor in both the radial and axial directions. The cell sizes gradually increase away from the dump plane. The grid resolution is the same as that used in our previous studies, where it was found to be sufficient to produce accurate results.[3] The time step used is $\Delta t = 3.76 \times 10^{-7}$ s. For these flow conditions the characteristic shedding frequency of vortex structures at the combustor step is given by $\sigma_s = 1380$ Hz. A vortex merging frequency of 690 Hz and an inlet acoustic mode of 145 Hz are additional characteristic frequencies observed in the system.

A Lagrangian approach is used to track each particle. Under the assumption that the density of the particle ρ_p is much larger than the density of the surrounding gas phase, the equations of motion for a particle of diameter d_p in the absence of gravity reduce to

$$\frac{\mathrm{d}\boldsymbol{V}(t)}{\mathrm{d}t} = \frac{[\boldsymbol{U}(\boldsymbol{Y}, t) - \boldsymbol{V}(t)] f(Re_p)}{\tau_p} \tag{4}$$

$$\frac{\mathrm{d}\boldsymbol{Y}(t)}{\mathrm{d}t} = \boldsymbol{V}(t) \tag{5}$$

where $\boldsymbol{Y}$ is the particle position, $\tau_p = \rho_p d_p^2/18\mu_{\text{gas}}$ is the particle response time, and μ_{gas} is the dynamic viscosity of the gas phase. The coefficient f is a scalar function of the particle Reynolds number Re_p, with $f(Re_p) = 1.0 + Re_p^{0.687}$. A fourth-order, predictor-corrector method is used to obtain particle velocity and position in time, and a sixth-order Lagrangian interpolation scheme is used to interpolate flow properties from the computational grid to the particle positions. Particle–particle interactions are neglected.

To take into account return effects from the dispersed particles to the gas phase, the particle momentum and energy are calculated for each particle location, and a linear weighting scheme based on cell volume is used to find the corresponding source terms used in Eqs. (2) and (3) for the gas-phase calculation at the surrounding

Presented as Paper 95-2561 at the AIAA/ASME/SAE/ASEE 31st Joint Propulsion Conference, San Diego, CA, July 10–12, 1995; received March 16, 1998; revision received Nov. 6, 1998; accepted for publication Nov. 19, 1998.

*Mathematician, Laboratory for Computational Physics and Fluid Dynamics, Code 6410. Member AIAA.

†Head, Center for Reactive Flow and Dynamical Systems, Laboratory for Computational Physics and Fluid Dynamics. Associate Fellow AIAA.

‡Professor, Department of Mechanical Engineering. Associate Fellow AIAA.